

NANO-OPTICS

PACS numbers: 78.67.Bf; 42.25.Fx; 42.25.Gy
DOI: 10.1070/QE2011v041n02ABEH014331

Optical antireflection of a medium by nanocrystal layers

A.S. Shalin

Abstract. **Optical properties of a semi-infinite dielectric medium comprising a monolayer quasi-crystal of nanoparticles are considered. It is shown that imbedding a single layer of nano-objects regularly distributed in space under certain conditions may provide close to 100 % transmission of the medium in a wide spectral range.**

Keywords: *metamaterial, nanoparticle monolayer, light scattering by small particles, antireflection.*

1. Introduction

Need in materials and media with a light transmission close to 100 % in a wide spectral range often arises in modern optics. Greater light transmission of a dielectric medium is usually achieved by depositing thin-film single- or multilayer interference coatings. This approach is applicable for a sufficiently wide spectral range; however, it has substantial limitations related to necessity of depositing a great number of films of various materials with a strictly specified thickness [1] and to optical properties of the latter [2, 3]. These factors limit the transparency to at most 99.8 % – 99.85 % [1]. A greater part of presently employed antireflection coatings has not so high transparency and exhibits dichroism as well [4]. In the infrared and microwave ranges, ferroelectrics and semiconductors have a sufficiently high refractive index, which hinders creation of antireflection coatings for them. Hence, a search for alternative antireflection methods capable of obtaining higher transmission in the visible spectral range becomes a necessity.

There is a series of works devoted to antireflection of materials due to a gradual variation in the refractive index at the medium – vacuum interface by creating an artificial roughness [5, 6]. However, practical employment of such structures is often impossible because of these irregularities. Interesting are antireflection coatings of artificial materials with adjusted properties [7 – 9]. The authors of [7] suggested a coating obtained by the sol gel method, which possesses enhanced optical properties. In [8, 9], a possible employment of such coatings was studied in applications with high-intensity laser radiation. However, it worth noting that most coatings obtained by the sol gel technology are distinguished by a weak attrition resistance, brittleness, and sufficiently high cost. For antireflection coating the authors of [10] suggested using the polymer film with imbedded metal oxide nanoparticles, whose refractive index may be varied in a wide range by changing the particle concentration. In this case, the antireflection spectrum has a pronounced peak character similarly to the case of an ordinary homogeneous coating.

Currently, a controlled growth and allocation of objects of nanometer dimensions on a surface of a substrate became possible, and the investigations aimed at creation of antireflection coatings in the form of a nanostructure deposited on a substrate surface are extensively developing [11 – 16]. In [17], it is shown that the reflective capability of the substrate with a 'nap' of SiO_2- and TiO_2-nanotubes deposited on it may be reduced to 0.05 % at certain wavelengths. A similar effect was also observed in arrays of carbon nanotubes [18] and is related to light 'trapping' in a sparse chaotic nanostructured material. Recently, subwavelength antireflection structures have been used for increasing the efficiency of such semiconductor optoelectronic devices as solar cells, light emitting devices, photodetectors, and for enhancing brightness of displays [15, 19 – 22]. In [23], the damping of reflection by an ordered nanocrystal was experimentally studied by the example of a periodical layer of nanocones placed on a lens surface. In [24], we theoretically predicted a possibility of obtaining total antireflection of a substrate at a prescribed wavelength by depositing on it an ordered layer of spherical nanoclusters. However, this effect was only obtained for some exotic weakly reflecting media.

In the present study, we investigate optical properties of the dielectric medium with a single-layer ordered nanocrystal imbedded into its near-surface region. Basing on our theoretical approach we show that the system exhibits an enhanced (up to 100 %) transparency, which may be selective (at a wavelength given *a priori*) or broadband without increasing the number of layers in the nanocrystal and using no coatings. The optical density of the medium is not a limiting factor and antireflection can be obtained for weakly or strongly refracting materials.

2. Principal equations

Let us consider a nanoaggregate shown in Fig. 1, which represents the quasi-crystalline single layer of nanoparticles with lattice parameters $\boldsymbol{a}_1$ and $\boldsymbol{a}_2$ imbedded into a dielectric

A.S. Shalin Ulyanovsk State University, ul. L. Tolstogo 42, 432700 Ulyanovsk, Russia; V.A. Kotel'nikov Institute of Radio Engineering and Electronics, Russian Academy of Sciences, Ulyanovsk Branch, ul. Goncharova 48, 432011 Ulyanovsk, Russia;
e-mail: shalin_a@rambler.ru

Received 2 April 2010; revision received 25 October 2010
Kvantovaya Elektronika **41** (2) 163 – 169 (2011)
Translated by N.A. Raspopov

medium in the field of external plane wave $\boldsymbol{E}_{\rm in} = \boldsymbol{E}_{0\rm in}\exp(\mathrm{i}\boldsymbol{k}_0\boldsymbol{r} - \mathrm{i}\omega t)$, where $\boldsymbol{k}_0$ is the wave vector. Extent of the layer and medium in the plane xy is assumed infinite and the origin of coordinates is taken, for convenience, on the surface of the medium-matrix so that the centre of certain particle has the radius vector $\boldsymbol{\Delta} = (0, 0, -\Delta)$. In the general case, the fields reflected and passed through a system can be presented as a vector sum of the external field $\boldsymbol{E}_{\rm in}$, the field of medium atoms $\boldsymbol{E}_{\rm P}$, and the fields scattered by nanoclusters $\boldsymbol{E}_{ij\,\rm sca}$, whose wave structure, in turn, is determined by the material, shape, and size of particles and by the incident local field:

$$\boldsymbol{E}(\boldsymbol{r}, t) = \boldsymbol{E}_{\rm in}(\boldsymbol{r}, t) + \boldsymbol{E}_{\rm P}(\boldsymbol{r}, t) + \sum_{i=-\infty}^{\infty}\sum_{j=-\infty}^{\infty}\boldsymbol{E}_{ij\,\rm sca}(\boldsymbol{r}, t). \qquad (1)$$

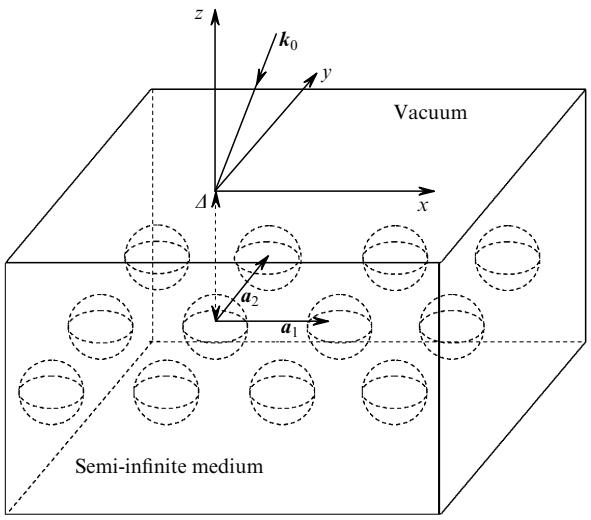

Figure 1. System geometry. External wave with the wave vector $\boldsymbol{k}_0$ passes from vacuum onto the surface of a semi-infinite medium inside which an ordered layer of nanoparticles parallel to the interface is placed; Δ is the depth of the nanocrystal layer position (the distance from the surface to the plane of nanoparticle centres).

Indices i and j determine the coordinate of a considered particle expressed in terms of lattice constants for the layer, the particle with the radius vector $\boldsymbol{\Delta}$ being zeroth. In the frameworks of the integral equation method that we have previously successfully used in investigating various nanostructure aggregates [24–27], the parameters $\boldsymbol{E}_{\rm P}$ and $\boldsymbol{E}_{ij\,\rm sca}$ can be written in the form

$$\boldsymbol{E}_{\rm P}(\boldsymbol{r}, t) = \int_V \mathrm{rot}\,\mathrm{rot}\frac{\boldsymbol{P}(\boldsymbol{r}', t - R/c)}{R}\,\mathrm{d}V',$$

$$\boldsymbol{E}_{ij\,\rm sca}(\boldsymbol{r}, t) = \frac{3}{4\pi}$$

$$\times\int_{V_j}\mathrm{rot}\,\mathrm{rot}\frac{\tilde{\varepsilon}_{ij}(\boldsymbol{r}'_{ij}) - \tilde{\varepsilon}_{\rm m}}{\varepsilon_{ij}(\boldsymbol{r}'_{ij}) + 2\tilde{\varepsilon}_{\rm m}}\frac{\boldsymbol{E}_{ij\,\rm eff}(\boldsymbol{r}'_{ij}, t - R_{ij}/c')}{R_{ij}}\,\mathrm{d}V'_{ij}, \qquad (2)$$

where $\boldsymbol{r}$ is the observation point; the medium-matrix is characterised by the polarisation $\boldsymbol{P}$, permittivity $\tilde{\varepsilon}_{\rm m}$, and refractive index $\tilde{n}_{\rm m} = \sqrt{\tilde{\varepsilon}_{\rm m}}$; $R = |\boldsymbol{r} - \boldsymbol{r}'|$ is the distance from an integration point $\boldsymbol{r}'$ inside the medium to the observation point; V is the volume of the medium; c is the speed of light in vacuum; the argument $(t - R/c)$ determines retardation of the corresponding parameter. Nanoparticles of the ensemble considered are characterised by the complex permittivities $\varepsilon_{ij}(\boldsymbol{r})$ and volumes V_{ij}; here $R_{ij} = |\boldsymbol{r} - \boldsymbol{r}'_{ij}|$, $\boldsymbol{r}'_{ij}$ is an integration point inside the nanoparticle with the coordinates i and j. The effective field $\boldsymbol{E}_{ij\,\rm eff}$ in (2) differs from the incident plane wave $\boldsymbol{E}_{\rm in}$ and is the wave acting on each point inside ijth nanoparticle with the allowance made for fields reradiated by other elements of the system. Here, we have $c' = c/\tilde{n}_{\rm m}$ for wave propagation inside the medium and $c' = c$ on the distance from the medium surface to the observation point if the latter resides in vacuum outside the system.

It worth noting that if the observation point is inside a nanoparticle, the effective field $\boldsymbol{E}_{ij\,\rm eff}$ splits into two components: the external component $\boldsymbol{E}'_{ij\,\rm eff}$ (acting on the considered object from outside) and internal $\boldsymbol{E}''_{ij\,\rm eff}$, which determines the interaction between atoms and conduction electrons from the nanocluster and is responsible for formation of permittivity. Taking into account the internal field leads to separation of expression (2) into local and nonlocal parts, which is thoroughly described in [28]; in this case, the local part reduces to the known Lorentz–Lorenz formula (for conducting nanoclusters, to its modification [29]) determining a relationship between the refractive index, polarisability, and concentration of constituting atoms. The boundary problem posed, thus, reduces to the solution of nonlocal equations comprising $\boldsymbol{E}'_{ij\,\rm eff}$.

For simplicity, we will assume that the monolayer consists of similar homogeneous spherical nanoclusters (with a nanoparticle radius $a_{ij} = a$, permittivity $\tilde{\varepsilon}_{ij}(\boldsymbol{r}'_{ij}) = \tilde{\varepsilon}$). In [24, 27], we considered light reflection from a monolayer of nanoparticles disposed on a substrate medium surface and suggested the method for solving analytically the system of integral equations (1), (2) with a high accuracy relative to a numerical *ab initio* solution [25, 26]. In the frameworks of that approach, placing the observation point at the centre of the zeroth particle $(i,j = 0)$ we obtain from (1), (2) the following expression for the effective optical field incident on the particle:

$$\boldsymbol{E}'_{00\,\rm eff}(\boldsymbol{\Delta}, t) = \alpha_p\hat{A}_p\boldsymbol{E}'_{00\,\rm eff}(\boldsymbol{\Delta}, t) + [\hat{R}_{21}\boldsymbol{E}_{\rm m}(0, t)$$

$$+ \hat{T}_{12}\boldsymbol{E}_{\rm in}(0, t)]_{\frac{(t - (\boldsymbol{k}_0\boldsymbol{\Delta})\tilde{n}_{\rm m}}{k_0 c}}, \qquad (3)$$

where the first summand characterises the field of the layer itself and second summand in square brackets is the external field falling onto the layer. Here, we have

$$\boldsymbol{E}_{\rm m}(0, t) = \alpha_p\hat{C}_p^{+}(-\boldsymbol{\Delta})\boldsymbol{E}'_{00\,\rm eff}(\boldsymbol{\Delta}, t). \qquad (4)$$

This is the field produced by the monolayer and passing to the interface from inside the medium. The polarisability of nanoparticles α_p in (3), (4) is calculated by the known formula for a small sphere with a prescribed local dielectric constant [30]:

$$\alpha_p = a^3\frac{\tilde{\varepsilon} - \tilde{\varepsilon}_{\rm m}}{\tilde{\varepsilon} + 2\tilde{\varepsilon}_{\rm m}}. \qquad (5)$$

Expressions (3), (4) allow for the fact that, since all clusters in the layer are in similar conditions we have $|\boldsymbol{E}'_{00\,\rm eff}| = |\boldsymbol{E}'_{ij\,\rm eff}| = |\boldsymbol{E}'_{\rm eff}|$. Describing an interaction of the complicated field emitted by the layer of nanoparticles with

the medium–vacuum interface we used tensors of Fresnel transmission and reflection coefficients $\hat{T}$ and $\hat{R}$ [24, 27]; in this case, the order of indices indicates the direction of the passing wave ('12' – from vacuum to medium, '21' – from medium to vacuum). The argument $t-(\boldsymbol{k}_0\boldsymbol{\Delta})\tilde{n}_{\mathrm{m}}/(k_0c)$ characterises the lag due to wave passing from the medium-matrix surface to the plane of nanoparticle centres. In the frameworks of this study we will assume that there is no intermediate layer near the surface, and the incident wave at the mathematical interface is substituted with passed one propagating at the speed $c/\tilde{n}_{\mathrm{m}}$, which corresponds to the cancellation theorem [28].

The phase shift of the field passing to other particles (nonzero particles with $i,j\neq 0$) can be found from the principle of parallel translation symmetry [24, 27]:

$$\boldsymbol{E}'_{ij\,\mathrm{eff}}=\boldsymbol{E}'_{00\,\mathrm{eff}}\exp(\mathrm{i}\boldsymbol{q}\boldsymbol{r}_{ij}), \tag{6}$$

where $\boldsymbol{r}_{ij}$ is the radius vector to the centre of ijth nanoparticle and $\boldsymbol{q}=(k_{0x},k_{0y},0)$.

As we and other authors [25, 26, 31–33] repeatedly mentioned earlier, the lattice sums $\hat{A}_p$ and $\hat{C}_p^{\pm}$ introduced in (3), (4) (which characterise the fields emitted by the monolayer of nanoparticles to an observation point residing, correspondingly, inside or outside the layer; the sign '+' means that the wave propagates in the positive direction of the z axis) actually do not converge in real space. This fact is explained by presence of weakly decaying terms proportional to $1/R$ in the expansion of a field scattered by a nanoparticle. Nevertheless, calculation of these parameters in the Fourier representation has no difficulties and is given, for example, in [32, 33]. In this case, the final expressions determining decomposition of the field scattered by the monolayer into a plane (zeroth) and other evanescent harmonics are rather awkward [24–27]. Note that this approach provides good agreement between the simulated spectra and results of accurate numerical calculations. In the present study, we will limit ourselves to the relationships for the zero non-evanescent terms, which will be needed in further analysis:

$$\begin{aligned}\hat{C}_p^{\pm}(-\boldsymbol{\Delta})&=\sum_{i,j=-\infty}^{\infty}\exp(\mathrm{i}\boldsymbol{q}\boldsymbol{r}_{ij})\,\mathrm{rot}\,\mathrm{rot}\left[\frac{\exp(\mathrm{i}k_0\tilde{n}_{\mathrm{m}}|\boldsymbol{r}_{ij}|)}{|\boldsymbol{r}_{ij}|}\right]\\&\approx\boldsymbol{C}_n\exp(\mp\mathrm{i}\boldsymbol{k}_0r\tilde{n}_{\mathrm{m}}),\end{aligned} \tag{7}$$

$$\begin{aligned}A_p^{x,y}&=\sum_{\substack{i,j=-\infty,\\ i,j\neq 0}}^{\infty}\exp(\mathrm{i}\boldsymbol{q}\boldsymbol{r}_{ij})\,\mathrm{rot}\,\mathrm{rot}\left[\frac{\exp(\mathrm{i}k_0\tilde{n}_{\mathrm{m}}|\boldsymbol{r}_{ij}-\boldsymbol{\Delta}|)}{|\boldsymbol{r}_{ij}-\boldsymbol{\Delta}|}\right]\\&\approx\frac{1}{3}\frac{2\sqrt{H}}{|\boldsymbol{a}_1\times\boldsymbol{a}_2|^{3/2}}[\,\mathrm{Im}\{B\}(3\pi+H)\\&\quad+\frac{2(\pi-H)\exp(H/4\pi)}{\sqrt{H}}+\mathrm{i}[H+\mathrm{Re}\{B\}(3\pi-H)]],\end{aligned} \tag{8}$$

where

$$\boldsymbol{C}_n=\frac{\boldsymbol{E}_{\mathrm{in}}}{|\boldsymbol{E}_{\mathrm{in}}|}\frac{2\pi\mathrm{i}k_0\tilde{n}_{\mathrm{m}}}{|\boldsymbol{a}_1\times\boldsymbol{a}_2|};\quad H=(k_0\tilde{n}_{\mathrm{m}})^2|\boldsymbol{a}_1\times\boldsymbol{a}_2|;$$
$$B=\mathrm{erfc}\left(\frac{\mathrm{i}\sqrt{H}}{2\sqrt{\pi}}\right), \tag{9}$$

and $\boldsymbol{a}_1$, $\boldsymbol{a}_2$ are the lattice constants for the layer.

By solving system (3), (4) we obtain the following expression for the field:

$$\boldsymbol{E}'_{00\,\mathrm{eff}}(\boldsymbol{\Delta},t)=\frac{\hat{T}_{12}\exp[\mathrm{i}\tilde{n}_{\mathrm{m}}(\boldsymbol{k}_0\boldsymbol{\Delta})]}{1-\alpha_p\hat{A}_p-\hat{R}_{21}\alpha_p\hat{C}_p^{+}(-2\boldsymbol{\Delta})}\boldsymbol{E}_{\mathrm{in}}(0,t), \tag{10}$$

where $\hat{C}_p^{+}(-2\boldsymbol{\Delta})$ makes allowance for the wave lagging on passing from the surface to the plane of nanoparticle centres and back.

Thus, in view of (4), the expression for the amplitude of the total wave reflected from the composite medium at the observation point $\boldsymbol{x}$ takes the form:

$$\begin{aligned}\boldsymbol{E}_{\mathrm{refl}}(\boldsymbol{x},t)=\Bigg[&\hat{R}_{12}\exp(\mathrm{i}\boldsymbol{k}_0\boldsymbol{x})+\hat{T}_{21}\alpha_p\hat{C}_p^{+}(\boldsymbol{x}-\boldsymbol{\Delta})\\&\times\frac{\hat{T}_{12}\exp[\mathrm{i}\tilde{n}_{\mathrm{m}}(\boldsymbol{k}_0\boldsymbol{\Delta})]}{1-\alpha_p\hat{A}_p-\hat{R}_{21}\alpha_p\hat{C}_p^{+}(-2\boldsymbol{\Delta})}\Bigg]\boldsymbol{E}_{\mathrm{in}}(0,t),\end{aligned} \tag{11}$$

where the first summand in parenthesis is responsible for the reflection from the surface of a clear medium without imbedded nanoparticle layer, and the second summand is the contribution of the layer into the total reflected field.

3. Imaginary boundary method

Expression (11) in some cases can be substantially simplified. In [27], we have shown that for the considered system in the optical spectral range one may retain only the first non-evanescent harmonics in the lattice sum $\hat{C}_p^{+}$ and, hence, employ approximate expressions (7)–(9) instead of the complete expansion [24–27, 29]. Then, assuming normal incidence for the external wave we may write the following expression:

$$\hat{r}=\frac{\boldsymbol{E}_{\mathrm{refl}}(0,t)}{\boldsymbol{E}_{\mathrm{in}}(0,t)}=\frac{\hat{R}_{12}+\hat{R}_{\mathrm{L}}\exp[2\mathrm{i}\tilde{n}_{\mathrm{m}}(\boldsymbol{k}_0\boldsymbol{\Delta})]}{1-\hat{R}_{21}\hat{R}_{\mathrm{L}}\exp[2\mathrm{i}\tilde{n}_{\mathrm{m}}(\boldsymbol{k}_0\boldsymbol{\Delta})]}, \tag{12}$$

which exactly corresponds to the Airy reflection coefficient for the film on a surface of the substrate medium, where

$$\hat{R}_{\mathrm{L}}=\frac{\alpha_p\boldsymbol{C}_n}{1-\alpha_p\hat{A}_p} \tag{13}$$

is the tensor of non-Fresnel reflection coefficients for the monolayer. Similarly, we can write the transmission coefficient for a system, which describes the total field passed into the medium-matrix:

$$\hat{t}=\frac{\boldsymbol{E}_{\mathrm{tran}}(\boldsymbol{\Delta},t)}{\boldsymbol{E}_{\mathrm{in}}(0,t)}=\frac{\hat{T}_{12}\hat{T}_{\mathrm{L}}\exp[\mathrm{i}\tilde{n}_{\mathrm{m}}(\boldsymbol{k}_0\boldsymbol{\Delta})]}{1-\hat{R}_{21}\hat{R}_{\mathrm{L}}\exp[2\mathrm{i}\tilde{n}_{\mathrm{m}}(\boldsymbol{k}_0\boldsymbol{\Delta}]}, \tag{14}$$

where the tensor of non-Fresnel transmission coefficients for the monolayer is

$$\hat{T}_{\mathrm{L}}=1+\frac{\alpha_p\boldsymbol{C}_n}{1-\alpha_p\hat{A}_p}. \tag{15}$$

Tensors (13) and (15) are similar because the field of the nanoparticle layer is symmetrical with respect to the plane in which it is arranged [see (7)].

Thus, the considered two-dimensional nanocrystal presents an imaginary infinitely thin (despite the fact that the particles have a finite dimension) interface between two

media, which crosses the centres of the clusters and possesses complicated reflection and transmission coefficients.

In Fig. 2, calculated reflection coefficients of the system $\Re = |\hat{r}|^2 \times 100\,\%$ are shown for two cases: $\tilde{n} > \tilde{n}_\mathrm{m}$ and $\tilde{n} < \tilde{n}_\mathrm{m}$; the reflective capability of a pure medium is 4 %. The distance Δ from the surface to the plane crossing the centres of nanoparticles is constant and equal to the radius of the latter. For comparison, the results of exact *ab initio* calculations performed for the considered structures by the finite element approach [34, 35] are also presented in the figures. Obviously, the numerical and analytical [obtained from (12)] dependences well agree, and the difference does not exceed 1 %.

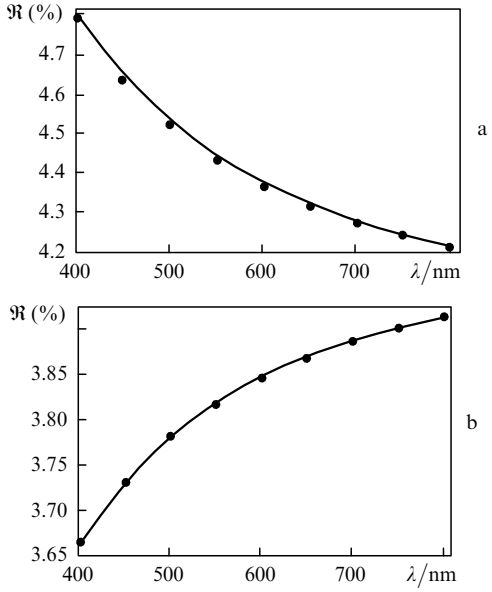

Figure 2. Spectral dependence of the reflection coefficient for the glass ($\tilde{n}_\mathrm{m} = 1.5$) comprising a layer of nanoparticles. A solid line is the calculation in the frameworks of the considered theory, points show results of the exact electrodynamic calculation by the finite element approach. Geometrical parameters of the structure are: the layer lattice is square in all cases $|\boldsymbol{a}_{1,2}| = 4a$, the depth of layer position is $\Delta = 10$ nm, a particle radius is $a = 10$ nm, the external field hereinafter is polarised along the y axis and falls to the system normally. The refractive index of nanoparticles is $n = 2.5$ (a) and $n = 1$ (b).

Note that in the considered system, either constructive (Fig. 2a) or destructive (Fig. 2b) interference may occur for the waves reflected from the real and imaginary interfaces, which makes it possible to vary the resulting transmission of the system in a wide range. This follows from the general physical reasons: imbedding a layer of nanoparticles having a greater real part of the refractive index than the medium-matrix has, makes the medium in that place more optically dense. Hence, the reflection from the imaginary interface occurs with the phase shifted by π [28] (as in the case of reflecting from a real interface) and, as is seen from (12), the reflected waves enhance each other. In the opposite case, the phase is not shifted and the amplitude of the wave reflected from the monolayer of nanoparticles is a positive value. Here one should make allowance for the depth of the nanoparticle layer position because it determines the phase shift $2\tilde{n}_\mathrm{m} \times (\boldsymbol{k}_0\Delta)$, which in the considered cases is well below unity.

4. Condition for medium antireflection by an embedded nanocrystal layer

Expression (12), in an explicit form known from the classical theory for antireflection coatings, determines the conditions in which the embedded quasi-crystal layer completely cancels the wave reflected from the system making the latter absolutely transparent. Assuming $\hat{r} = 0$ in (12) we may write

$$\hat{R}_{12} = -\hat{R}_\mathrm{L} \exp[2\mathrm{i}\tilde{n}_\mathrm{m}(\boldsymbol{k}_0\Delta)], \tag{16}$$

where the left-hand side characterises the medium-carrier, and the right-hand side refers to the nanocrystal. Note that earlier we studied the phenomenon of total optical antireflection for a substrate medium due to depositing on its surface a monolayer of nanoparticles [24]. The effect could only be realised in the narrow range of the substrate refractive index values close to unity, which is explained by low reflecting capability of the monolayer in vacuum [27] and by the small value of the parameter $2a$ (the path difference for the waves reflected from the monolayer and from substrate in the case where the particles reside on the surface) as compared to $\lambda/2$ (λ is the wavelength of the incident radiation). If such a monolayer with similar material and geometrical parameters is embedded into a medium, its reflective capability falls because the polarisability of nanoparticles α_p falls (5) (obviously, the reflecting capability is less at smaller difference between the refractive indices of the medium and particles). Nevertheless, the possibility to vary the depth of layer position gives a chance to exactly satisfy the interference minimum condition imposed on the path difference for the waves reflected from the real and imaginary interfaces. The non-Fresnel reflective index $\hat{R}_\mathrm{L}$ is a complex value even in the case of dielectric nanoparticles [see (7)–(9)] and relationship (16) can tentatively be divided into two components:

$$|\hat{R}_{12}| = |\hat{R}_\mathrm{L}|, \tag{17a}$$

$$\exp[2\mathrm{i}\tilde{n}_\mathrm{m}(\boldsymbol{k}_0\Delta) + \mathrm{i}(\rho_\mathrm{L} - \rho_{12}) + \mathrm{i}\pi] = -1, \tag{17b}$$

where ρ_{12} and ρ_L are the arguments of $\hat{R}_{12}$ and $\hat{R}_\mathrm{L}$, respectively. Since the medium we work with is a dielectric with the refractive index $\tilde{n}_\mathrm{m} > 1$ it is obvious that $\rho_{12} = \pi$. Thus, the interference is destructive in the two cases (with the accuracy of up to $2\pi N$, where N is an integer):

$$\tilde{n} > \tilde{n}_\mathrm{m}, \quad \frac{\pi}{2} \leqslant 2\tilde{n}_\mathrm{m}(\boldsymbol{k}_0\Delta) + \rho_\mathrm{L} \leqslant \frac{3\pi}{2}; \tag{18a}$$

$$\tilde{n} < \tilde{n}_\mathrm{m}, \quad -\frac{\pi}{2} \leqslant 2\tilde{n}_\mathrm{m}(\boldsymbol{k}_0\Delta) + \rho_\mathrm{L} \leqslant \frac{\pi}{2}. \tag{18b}$$

Note that employment of metal nanoparticles whose real part of the refractive index is less than unity might substantially increase the parameter $|\hat{R}_\mathrm{L}|$ and, respectively, antireflect optically more dense media. However, absorption of radiation in such a quasi-crystal may reach several percent, which makes its employment unreasonable.

Employment of dielectric (or weakly conducting) nanoparticles with the refractive index greater than that of the medium to be antireflected (18a) provides, in some cases, higher reflecting capability of the monolayer, because in a

transparent dielectric media (such as glass, optical polymers etc.) polarisability for the particles with $\tilde{n} > \tilde{n}_m$ may be several times greater than for particles of the same dimension with $\tilde{n} < \tilde{n}_m$. As was already mentioned the polarisability α is proportional to the difference $\tilde{n}^2 - \tilde{n}_m^2$ (5) and takes the greatest absolute values at $\tilde{n} = 1$ (which corresponds to the layer of nanocavities and is the minimal refractive index for non-metallic nanoinclusions) and at $\tilde{n} = \tilde{n}_{max}$, which corresponds to the maximal possible refractive index for existing nonmetals. Since $|\tilde{\varepsilon}_{max} - \tilde{\varepsilon}_m| \gg |1 - \tilde{\varepsilon}_m|$ it is obvious that

$$\frac{|\alpha_p(\tilde{\varepsilon}_{max})|}{|\alpha_p(1)|} \gg 1. \tag{19}$$

For example, for a nanocavity and silicon nanoparticle of the same dimension imbedded into a glass ($\tilde{n}_m = 1.5$), ratio (19) is approximately three over the total visible range.

In Fig. 3, the reflection coefficient $\Re$ of a glass matrix with an imbedded quasi-crystal layer of silicon nanoparticles is shown. The dispersion dependence of the complex refractive index of particles $\tilde{n}(\lambda)$ we take equal to that of a bulk material [36] neglecting the size effect. By transmission here and in what follows is meant a percent fraction of the light wave energy passed into the medium less the energy absorbed by the layer. In the considered case the transmission coefficient is $\Im = 100\,\% - \Re$ because the absorption is rather small (since both the layer width and imaginary part of the refractive index for silicon are small) and does not exceed 10^{-5} %, so we can neglect it.

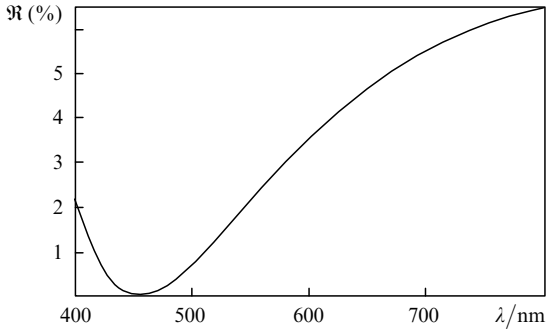

Figure 3. Reflection coefficient of glass ($\tilde{n}_m = 1.5$) with an imbedded layer of silicon nanoparticles of radius $a = 17$ nm. The lattice constants are similar and equal to $3a$, the depth of the layer position is $\Delta = 110$ nm; experimental data on the refraction index for silicon are taken from [36].

The reflection coefficient in the minimum observed at the wavelength of 457 nm (the refractive index for silicon is $\tilde{n}_{Si} = 4.6 + i0.1$) equals 0.02 % and, respectively, the transmission coefficient is $\Im = 99.98$ % with an accuracy of 10^{-3}. The spectral dependence in this case has a pronounced peak and the reflection outside the minimum noticeably exceeds that of a pure medium. This fact is not surprising if we recall that a quasi-crystal layer of the nanoparticles with $\tilde{n} > \tilde{n}_m$ embedded into the matrix increases the optical density of the system. Moreover, in the considered spectral range under certain conditions (for example, at large nanoparticle dimensions), an interference maximum of reflection may be observed, which also impedes a wide-band antireflection of the medium-matrix. Thus, employment of nanoparticles with the refractive index greater than that of the medium-carrier is only reasonable if we need a high transmission for radiation at a prescribed wavelength, for example, in creating light filters or in optical devices for monochromatic radiation.

From (17) we may determine conditions, under which a wideband antireflection of the medium is achieved. Note that in the case of a film interference coating, conditions (17a) and (17b) can be simultaneously satisfied only at a certain wavelength. This is caused by the fact that keeping the phase factor constant (17b) and satisfying the condition for an interference minimum of reflection in a wavelength interval is only possible at the presence of the dispersion of the refractive index of the antireflection film or of the medium to be antireflected. This, in turn, breaks equality (17a) in the considered spectral range. Hence, multilayer coatings are used for wideband antireflection.

One may get over this difficulty by taking a nanocrystal as an antireflection agent. In that case, it is required that the phase shift ρ_L of the field reflected from the layer of nanoparticles be greater at longer wavelengths, thus, compensate a reduction of $2\tilde{n}_m(\boldsymbol{k}_0\boldsymbol{\Delta})$. The explicit form of the dependence of ρ_L on λ cannot be determined because the wavelength is comprised in relationships (7)–(9), (13) in a complicated form including terms containing the additional probability integral erfc. Nevertheless, basing on the mentioned formulae one can determine principal physical factors affecting behaviour of function $\rho_L(\lambda)$.

By substituting expressions (7)–(9) into (13) and expanding the result to the second infinitesimal term at $H \to 1$ (because at nanoparticle dimension and separation between them of several tens of nanometers this parameter varies in the visible range approximately from 0.15 to 1.9) we arrive at the following expression:

$$\rho_L \approx \arctan\left[-0.155 + \left(0.683 - \frac{|\boldsymbol{a}_1 \times \boldsymbol{a}_2|^{3/2}}{2\alpha_p\pi}\right)\frac{1}{\sqrt{H}} - 0.191\sqrt{H} - 0.188H\right] + \mathrm{sgn}[\tilde{n} - \tilde{n}_m]\pi. \tag{20}$$

From (20) it follows that ρ_L rises only if the factor at $H^{-1/2}$ is positive and $||\boldsymbol{a}_1 \times \boldsymbol{a}_2|^{3/2}/(2\alpha_p\pi)| > 1$ even at the minimal values of lattice constants $|\boldsymbol{a}_1| = |\boldsymbol{a}_2| = 2a$, because α_p/a^3 is always less than unity [see (5)]. Thus, for increasing ρ_L at greater wavelengths it is necessary that the polarisability of nanoparticles be negative, which is the case, for example, of $\tilde{n} < \tilde{n}_m$. A similar result may be obtained from investigating the sign of the derivative of ρ_L (20) with respect to wavelength.

In Fig. 4, dependences of $\rho_L(\lambda)$ are shown obtained by a numerical simulation from formula (13) for the cases $\tilde{n} > \tilde{n}_m$ (Fig. 4,a) and $\tilde{n} < \tilde{n}_m$ (Fig. 4,b). As was mentioned the character of the spectrum $\rho_L(\lambda)$ is determined by the sign of nanoparticle polarisability, in this case the dependence of $\tan[\rho_L(\lambda)]$ on the wavelength (Fig. 4,c) is almost linear, which follows from (20) as well.

Let us consider optical properties of a glass with an embedded layer of the spherical nanoinclusions satisfying condition (18b). For increasing the reflecting capability of the nanocrystal we assume it consisting of nanocavities with $\tilde{n} = 1$ having an increased radius of 50 nm with the lattice constants reduced to the minimal value corresponding to fully contacting cavities. The depth of the layer position we approximately determine from condition (17b) at the wave-

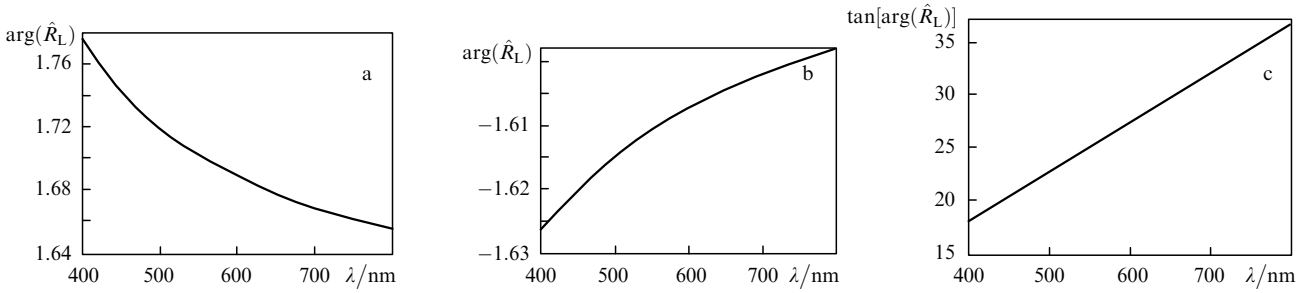

Figure 4. Spectral dependence of the wave phase shift (a, b) and tangent of it (c) in reflecting from a layer of nanoparticles. The layer is inside glass ($\tilde{n}_m = 1.5$). The lattice parameters are $|\boldsymbol{a}_{1,2}| = 4a$, the parameters of nanoparticles are: silicon, $\tilde{n} = \tilde{n}(\lambda)$ [36], $a = 15$ nm (a); air, $\tilde{n} = 1$, $a = 15$ nm (b, c).

length of 550 nm. The reflection coefficient will be calculated by using the exact finite element method [35] because, as we have shown in [27], for the given geometrical parameters of the nanoaggregate the theoretical approach described in the present paper can only be applied to estimation purposes.

As is seen from Fig. 5, medium antireflection in this case is actually wideband and the transmission coefficient is above 99 % in the interval 400 – 750 nm. The spectral range of transmission in which it weakly depends on a wavelength and is close to the maximal value (100 % at the wavelength of 527 nm) is also sufficiently wide ($\Im > 99.8$ % in the range 470 – 600 nm), which is explained by the mutual compensation of the phase shifts $2\tilde{n}_m(\boldsymbol{k}_0\boldsymbol{\Delta})$ and ρ_L. Note that in the blue range the transmission rapidly falls because the reflecting capability of the nanocavity layer rising at smaller wavelengths becomes too large. Hence, nanocavities of large size are suitable in more dense optical media than glass, because $|\hat{R}_L|$ in this case additionally rises.

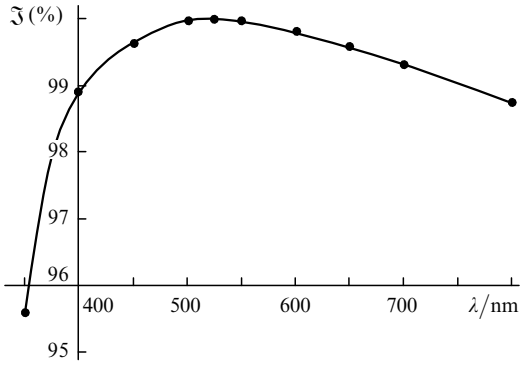

Figure 5. Transmission coefficient for glass ($\tilde{n}_m = 1.5$) with an imbedded layer of nanocavities of radius $a = 50$ nm. The lattice constants are similar and equal to $2a$ (the cavities are arranged tightly to each other), the depth of the layer position is $\Delta = 51$ nm. The calculation is performed by the finite element approach.

5. Conclusions

In this work, we study optical properties of the nanocomposite structure that is presented by a quasicrystal layer of nanoparticles imbedded into a semi-infinite medium-carrier. A theoretical approach is suggested, which interprets the ordered nanocrystal as an imaginary, infinitely thin interface possessing non-Fresnel reflection and transmission coefficients and allows one to use the known Airy formalism developed for a system 'film on a substrate'. Here, a transfer to the classical Airy description does not necessitate additional approximations or averaging of the parameters and fields over the volume of film, but allows one to deal with microscopic fields. For the first time, the conditions for total wideband antireflection of a system have been obtained and studied. It is shown, that a single monolayer of particles imbedded into a medium-carrier increases the transmission coefficient of the system to the values close to 100 % in a wide range of wavelengths. This is explained by the fact that the phase shift due to reflection from the nanocrystal may partially compensate the phase shift due to the wave path difference $2\tilde{n}_m(\boldsymbol{k}_0\boldsymbol{\Delta})$ at a changed wavelength, which, in turn, allows one to approximately satisfy the condition of reflection interference minimum in a certain spectral interval.

The results obtained may have wide application importance in developing materials with enhanced transparency ('invisible' materials), optical antireflection of systems, and for creating highly-transparent narrow-band light filters. Antireflection of existing artificial media with the refractive index close to unity is one more possible application of the phenomenon discovered [37]. According to the general theory of constructing antireflection coatings [28], the refractive index of an antireflection film in this case should be even closer to that of vacuum, which obviously prevents employment of natural materials for these purposes. Employment of a sparse nanostructure with controlled optical properties, which is just the case of a monolayer of nanoparticles or nanocavities substantially reduces and even eliminates reflection from such a material.

References

1. Visimax Technologies, Twinsburg, Ohio, http://visimaxtechnologies. com/anti-reflection-visiclear/.
2. Walheim S., Schaffer E., Mlynek J., Steiner U. *Science*, **283**, 520 (1999).
3. Lalanne P., Morris G.M. *Nanotechnology*, **8**, 53 (1997).
4. Koenig G.A., Niejelow N.G. United States Patent No. US 7, 311,938 B2, 25.12.2007.
5. Chen Y.W., Han P.Y., Zhang X.-C. *Appl. Phys. Lett.*, **94**, 041106 (2009).
6. Bruckner C., Pradarutti B., Stenzel O., Steinkopf R., et al. *Opt. Express*, **15**, 779 (2007).
7. Oliveira P.W., Krug H., Frantzen A., Mennig M., Schmidt H.K. *Sol–Gel Optics IV*. Ed. by B.S. Dunn, et al. (San Diego, CA: SPIE, 1997).
8. Pegon P.M., Germain C.V., Rorato Y.R., Belleville P.F., Lavastre E. *Proc. SPIE Int. Soc. Opt. Eng.*, **5250**, 170 (2004).
9. Floch H.G. Belleville P.F. *Proc. SPIE Int. Soc. Opt. Eng.*, **3136**, 275 (1997).

10. Krogman K.C., Druffel T., Sunkara M.K. *Nanotechnology*, **16**, S338 (2005).
11. Huang Y.-F., Chattopadhyay S., Jen Y.-J., Peng C.-Y., Liu T.-A., Hsu Y.-K., Pan C.-L., Lo H.-C., Hsu C.H., Chang Y.H., Lee C.-S., Chen K.-H., Chen L.-C. *Nat. Nanotechnology*, **2**, 770 (2007).
12. Li Y., Zhang J., Zhu S., Dong H., Wang Z., Sun Z., Guo J., Yang B. *J. Mater. Chem.*, **19**, 1806 (2009).
13. Wang S., Yu X.Z., Fan H.T. *Appl. Phys. Lett.*, **91**, 061105 (2007).
14. Gombert ff., Glaubitt W., Rose K., Dreibholz J., Blasi B., Heinzel A., Sporn D., Doll W., Wittwer V. *Thin Solid Films*, **351**, 73 (1999).
15. Wu Z., Walish J., Nolte A., Zhai L., Cohen R.E., Rubner M.F. *Adv. Mater.*, **18**, 2699 (2006).
16. Koo H.Y., Yi D.K., Yoo S.J., Kim D.-Y. *Adv. Mater.*, **16**, 274 (2004).
17. Xi J.-Q., Schubert Martin F., Kim Jong Kyu, et al. *Nature Photonics*, **1**, 176 (2007).
18. Garcia-Vidal Francisco J. *Nature Photonics*, **2**, 215 (2008).
19. Kanamori Y., Ishimori M., Hane K. *IEEE Photon. Technol. Lett.*, **14**, 1064 (2002).
20. Ishimori M., Kanamori Y., Sasaki M., Hane K. *Jpn. J. Appl. Phys.*, **41**, 4346 (2002).
21. Song Y.M., Choi E.S., Yu J.S., Lee Y.T. *Opt. Express*, **17**, 20991 (2009).
22. Yu P., Chang C.-H., Chiu C.-H., Yang C.-S., Yu J.-C., Kuo H.-C., Hsu S.-H., Chang Y.-C. *Adv. Mater.*, **21**, 1618 (2009).
23. Takashi Yanagishita, Kazuyuki Nishio, Hideki Masuda. *Appl. Phys. Express*, **2**, 022001 (2009).
24. Shalin A.S., Moiseev S.G. *Kvantovaya Elektron.*, **39**, 1175 (2009) [*Quantum Electron.*, **39**, 1175 (2009)].
25. Shalin A.S. *Pis'ma Zh. Eksp. Teor. Fiz.*, **90**, 279 (2009).
26. Shalin A.S. *Radiotekh. Elektron.*, **54**, 733 (2009).
27. Shalin A.S. *Opt. Spektrosk.*, **106**, 1029 (2009).
28. Born M., Wolf E. *Principles of Optics* (London: Pergamon, 1970; Moscow: Nauka, 1973).
29. Shalin A.S. *Fiz. Metal. Metalloved.*, **110**, 125 (2010).
30. Bohren C F, Huffman D R. *Absorption and Scattering of Light by Small Particles* (New York: Wiley, 1983; Moscow: Nauka, 1983).
31. Sukhov S.V., Krutitsky K.V. *Phys. Rev. B*, **65**, 115407 (2002).
32. Poppe G.P.M., Wijers C.M.J., Silfhout A. *Phys. Rev. B*, **44**, 7917 (1991).
33. Wijers C.M.J., Poppe G.P.M. *Phys. Rev. B*, **46**, 7605 (1992).
34. Arfken G.B., Weber H.J. *Mathematical Methods for Physicists* (New York: Acad. Press, 1995).
35. COMSOL Multiphysics 3.4, COMSOL AB, Stockholm, Sweden, http://www.comsol.com/ products/multiphysics/
36. Palik E.D. *Handbook of Optical Constants of Solids* (New York: Acad. Press, 1985).
37. Xi J.-Q., Kim Jong Kyu, Schubert M.F., Ye Dexian, Lu T.-M., Lin Shawn-Yu, Juneja Jasbir S. *Opt. Lett.*, **31**, 601 (2006).